JOURNAL OF SOLID STATE CHEMISTRY 81, 208–216 (1989)

Synthesis and Properties of $NdNiO_3$ Prepared by Low-Temperature Methods

JOHN K. VASSILIOU, MARC HORNBOSTEL, ROBIN ZIEBARTH, AND F. J. DISALVO*

Department of Chemistry, Cornell University, Ithaca, New York 14853

Received February 3, 1989

$NdNiO_3$ has been prepared with a rhombohedral perovskite structure by low-temperature methods, and its magnetic and electric properties have been studied between 4 and 300 K. The temperature coefficient of the resistivity changes at 130 K from positive (i.e., metal-like) to negative (i.e., semiconductor-like), with some thermal hysteresis at this "transition." The magnetic susceptibility shows Curie–Weiss behavior, modified by the changing thermal occupation of the Nd^{3+} crystal field levels, over the whole temperature range. Differential thermal analysis and thermogravimetric analysis showed oxygen loss beginning at 900°C in an N_2 atmosphere. Subsequent X-ray analysis at room temperature showed the presence of Nd_2NiO_4 and NiO. The electrical resistivity of sintered polycrystalline samples (1.5×10^{-2} ohm cm at 300 K) is somewhat above the expected minimum metallic conductivity, but the observation of a positive constant term in the susceptibility above 100 K suggests metallic band behavior. The hysteresis near 130 K suggests a structural distortion at low temperatures.

Introduction

Considerable interest in conducting oxides has been generated by the discovery of high-temperature superconductivity in some copper-oxide-based compounds. Metallic conductivity is quite uncommon in oxides and only a few of those are in fact superconductors. Since the mechanism for high-temperature superconductivity is as yet not agreed to, experimental studies of conducting oxides in general may help in our understanding of the necessary conditions for superconductivity and may result in further discoveries of new phenomena. Since the known metallic oxides occur mostly in compounds of the transition metals, we have initiated a study of such oxides. Here we report the properties of a new nickel oxide, $NdNiO_3$.

In most nickel oxide compounds nickel is divalent; however, there are a few compounds where Ni adopts a higher oxidation state. These are mostly rare-earth or alkaline earth ternary metal oxides. Among these compounds $LaNiO_3$, a rhombohedrally distorted pervoskite phase, is known to be a narrow band metallic conductor. Nickel compounds with Ni formal valency higher than two are usually unstable at high temperatures. Their synthesis, if possible, should therefore take place at low temperatures.

A number of authors (*1–3*) have reported

* To whom correspondence should be addressed.

0022-4596/89 $3.00

the preparation of $RNiO_3$ compounds (R = rare-earth element) involving high temperatures and atmospheric or high oxygen pressures. $LaNiO_3$ has been synthesized at 1 atm oxygen pressure and at 600°C. The other rare-earth compounds, isotypical to $LaNiO_3$, have been synthesized at 950°C and 60 kbar pressure from mixtures of (R_2O_3) rare-earth oxides, NiO, and $KClO_3$. The decomposition of $KClO_3$ provided the necessary oxygen atmosphere. This reaction does not take place at atmospheric pressure and 950°C; rather, R_2NiO_4 compounds with the K_2NiF_4 structure usually result (*4*). The electrical properties of these rare-earth phases, with the exception of $LaNiO_3$, have not been measured.

We report here the preparation of $NdNiO_3$ at 650°C and at atmospheric pressure using low-temperature preparatory methods (*5*). The structure of $NdNiO_3$ is similar to the structure of perovskites with a rhombohedral distortion (*2, 6*).

Methods of Preparation

The samples were prepared using two methods: decomposing well-mixed solid nitrates and a sol–gel precipitation decomposition process.

For the preparation involving solid nitrates, stoichiometric quantities of Nd_2O_3 and NiO of high purity were mixed together and dissolved in concentrated nitric acid. The excess nitric acid was removed by gentle heating. The remaining powder was slowly heated to 400°C for 1 hr. At that temperature the intimately mixed nitrates decomposed and the initially green powders turned black. Pellets of this material were cold-pressed at 4 kbar and heated to 650°C for 120 hr in an alumina crucible in an oxygen atmosphere.

In the sol–gel method, we started with aqueous solutions of the metal nitrates and a mixture of citric acid and ethylene glycol, in a ratio of 10 g citric acid to 4 ml ethylene glycol and 4 g metal nitrates. The above ingredients were mixed together and drops of HNO_3 were added to catalyze gel formation. The excess nitric acid was boiled off and the gel was decomposed by further heating to 400°C. The remaining black powder was cold pressed to 4 kbar and heated to 650°C for 120 hr in an alumina crucible in an oxygen atmosphere.

The resulting ceramic materials, obtained by either of the above methods, are black single-phase materials with high electrical conductivity.

Other preparation methods were attempted, including reaction of well-ground oxides and coprecipitation and rapid evaporation. However, sufficient mixing was apparently not achieved by either method and even after extended heating, multiphase products usually resulted.

Crystal Structure

X-ray diffraction patterns were taken at room temperature using a Sintag XDS-2000 powder diffractometer and Cu$K\alpha$ radiation. Si was used as an internal standard. The diffraction pattern of $NdNiO_3$ (Table I) is similar to the pattern of $LaNiO_3$, suggesting that the crystal symmetry is rhombohedral $R\text{-}3c$ (or hexagonal D_{3d}^6). The structure is a rhombohedrally distorted cubic perovskite. Since the tolerance factor, t, in the Goldsmith relation (*7, 8*) is $t = 0.85$, the rhombohedral distortion is expected. Note, however, that the structure and peak intensities are different from the orthorhombic cell reported for the phase prepared at high pressure (*3*).

The diffraction peaks are broad (e.g., 0.5° FWHM at 47.5° 2θ) and the width increases with increasing 2θ. Such broadening is consistent with small grain sizes of approximately 175 Å. These small sizes are likely a result of the low-temperature preparation methods used to prepare the material. Other factors which could contribute to the

TABLE I

$(h\ k\ l)_{rhom}$	$(h\ k\ l)_{hex}$	d(obs)	Relative intensity
1 1 0	0 1 2	3.79	10
1 0 −1	1 1 0	2.72	100
2 1 1	1 0 4		
2 2 0	2 0 4	1.91	35
1 1 −2	3 0 0		
2 −1 −1	2 1 4	1.567	25
3 1 0	0 1 8		
3 2 0	2 1 5		
3 3 1	2 0 7	1.465	5
3 3 3	0 0 9		
2 0 −2	2 2 0	1.356	8
4 2 2	2 0 8		
3 2 −1	1 3 4	1.210	5
4 3 1	1 2 8		
4 0 0	4 0 4	1.100	8

Note. The lattice parameters of $NdNiO_3$ for the rhombohedral and the equivalent hexagonal unit cell are given along with the appropriate miller indices and the observed peak intensity. Since the lines are broadened due to the small particle size, the line splittings due to the rhombohedral distortion are not directly observed. Rather the splitting is estimated from the excess width of multiple peaks over that estimated using the width calculated from the single (220) peak. Hexagonal lattice parameters, a = 5.44, c = 13.17; rhombohedral parameters, a = 5.40, α = 60.5°; pseudocubic cell, a = 3.85.

broadening include small differences in stoichiometry across the sample, crystalline defects, and frozen in mechanical strains. This broadening makes an exact determination of the rhombohedral distortion difficult. Our best estimate for the rhombohedral angle is 60.5 ± 0.2°. The dimensions of the resulting rhombohedral and its equivalent triple hexagonal unit cell are given in Table I.

Since the rhombohedral angle of the primitive cell (α = 60.5) is close to 60.0° (60° is the rhombohedral angle of the primitive cell derived from a face-centered cubic lattice), the X-ray pattern of $NdNiO_3$ can be approximately indexed in a cubic system. The unit cell length of the cubic pseudocell is a = 3.85 Å. The d-spacing and the observed intensities are also given in Table I. The (hkl) indices were assigned on the basis of the rhombohedral and hexagonal cells.

Thermal Analysis

Differential thermal analysis (DTA) and thermogravimetric analysis (TGA) were performed on the samples, using a Perkin–Elmer DTA–TGA thermal analysis system. The gas flow was 30 cm^3/min and the heating rate was 20°/min. Upon heating in an O_2 or N_2 atmosphere, an endothermic DTA peak appears, signaling the transformation of $NdNiO_3$ into a new phase. In a pure N_2 atmosphere, the onset temperature for the reaction is 900°C and the peak temperature is 960°C, while in a pure O_2 atmosphere the peak temperature has shifted to 1050°C.

Thermogravimetric analysis in a N_2 atmosphere demonstrates that the above transformation is accompanied by oxygen loss. Upon heating, the recorded TGA pattern shows a rapid loss of oxygen, starting at about 900°C, and achieving maximum rate of weight loss at 980°C. After completion of the thermal cycle, the products of the reaction were examined by X-ray analysis. The X-ray powder pattern shows a mixed-phase pattern, composed of NiO and Nd_2NiO_4 phases. Nd_2NiO_4 has tetragonal symmetry with the K_2NiF_4 structure (*4*). The reaction that takes place is:

$$2NdNiO_3 \xrightarrow[950°C]{N_2} Nd_2NiO_4 + NiO + \tfrac{1}{2}O_2.$$

At higher temperatures, in analogy with La_2NiO_4 (*9*), it is expected that Nd_2NiO_4 will decompose to the constituent oxides according to the reaction:

$$Nd_2NiO_4 \rightarrow Nd_2O_3 + NiO.$$

However, DTA experiments up to 1300°C did not show any sign of further decomposition.

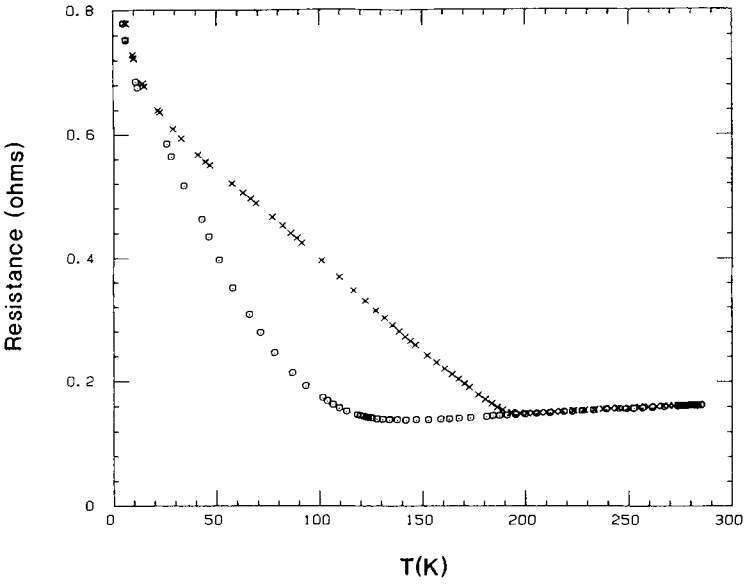

FIG. 1. Resistance versus temperature. The resistance shows a minimum near 120 K and thermal hysteresis at low temperatures.

Resistance Measurements

The resistance of the samples was measured by the four-probe method. Rectangular samples, cut from a pellet sintered at 650°C in O_2, were used for the electrical resistance measurements. The sample dimensions were roughly 10 × 2 × 2 mm. Four wires were bonded to the samples by conducting silver paint and baked at 100°C for 2 hr. The resistance of the contacts was less than the sample resistance, and their ohmic behavior was confirmed by testing the linearity of the current–voltage characteristics. The room-temperature measured resistivity is 1.5×10^{-2} ohm cm. Due to the size of the contacts this value has a rather large uncertainty of about 25%. The temperature dependence of the resistance is given in Fig. 1. In the temperature range between 130 and 300 K, the behavior is metallic-like. At lower temperatures the behavior changes smoothly to semiconducting-like; the resistivity increases rapidly with decreasing temperature. Upon heating, the temperature dependence of the resistance follows a similar thermal pattern but with a large and repeatable hysteresis. The hysteresis appears the same independent of the cooling or heating rate, over rates of 0.5 to 5 K/sec.

In polycrystalline materials, the grain boundaries and the coupling between the grains may affect the transport properties of the samples significantly. In order to examine the effect of the grain boundaries on the temperature dependence of the resistance, we measured the resistance of samples prepared under different pressure and temperature conditions. Pellets were annealed at 600°C in an oxygen atmosphere under uniaxial stress of approximately of 0.5 kbar. The temperature dependence of the resistance of the samples prepared this way does not show any measurable change from that shown above. While this suggests that grain boundary effects do not dominate the measured electrical properties, only a

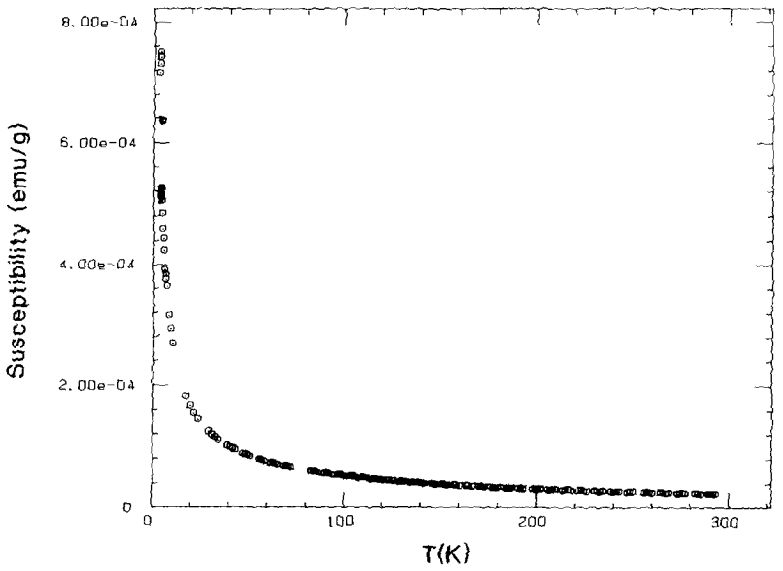

FIG. 2. Magnetic susceptibility versus temperature.

single-crystal measurement can be conclusive.

Magnetic Measurements

The magnetic susceptibility of the sample was measured between 4.2 and 300 K by the Faraday method, at a magnetic field strength of 10 kG. The field gradients at different fields were calibrated by using $HgCo(SCN)_4$ as a standard (16.44×10^{-6} emu/g at 293 K).[1] This calibration was checked using several pure metals. Our measured values and literature values are (all in units of 10^{-6} emu/g): Hg, measured = -0.165, literature = -0.167 (*10*); Ta, measured = 0.859, literature = 0.851 (*10*) and 0.849 (*10*). We take these differences to estimate our absolute accuracy and conservatively quote +/−2% absolute error on the value of the obtained susceptibility. The relative precision with which changes in the susceptibility with temperature can be measured depends upon the sample size and its susceptibility, but in this case the precision is better than 0.1%.

The susceptibility, X, of $NdNiO_3$ at room temperature was independent of the applied magnetic field from 2 to 15 kg. This indicates that no ferromagnetic impurities contaminated the sample (*11*). The results of the temperature-dependent measurements are plotted in Fig. 2. The higher temperature data are better illustrated in a plot of the inverse susceptibility vs temperature (Fig. 3). At room temperature, the susceptibility is 2.25×10^{-5} emu/g, typical of a paramagnetic substance with a large concentration of local magnetic moments. At lower temperatures, the susceptibility increases, displaying paramagnetic Curie–Weiss behavior.

In simple cases, the data might be expected to fit the Curie–Weiss equation

$$X = C/(T + T_c) + X_0,$$

where C and T_c are the Curie constant and Curie temperature, respectively. X_0 is usu-

[1] For $HgCo(NCS)_4$, see Ref. (*10a*). For the other standards see the "Handbook of Chemistry and Physics" (*10b*) or Ref. (*10c*).

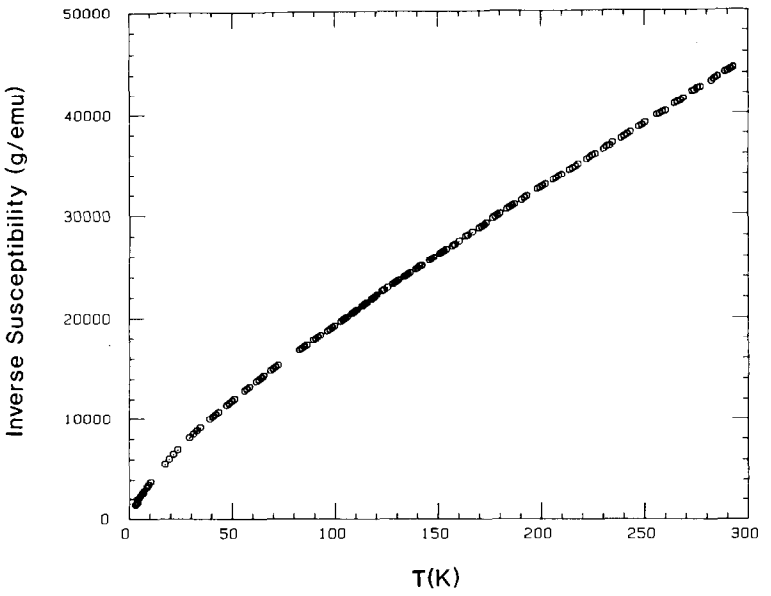

FIG. 3. The inverse susceptibility versus temperature shows the high-temperature data better.

ally a constant which includes the Pauli–Landau paramagnetic susceptibility, the core diamagnetic susceptibility, and the Van Vleck susceptibility. However, in this case the Curie "constant" is temperature dependent due to crystal field splitting of the $J = 9/2$ ground state. To first order we might estimate the magnitude of the crystal field by comparison to other Nd oxides. The susceptibility of Nd_2O_3 shows a deviation from simple Curie–Weiss behavior below about 80 K (*12*) as the crystal field levels become thermally depopulated.

Since the crystal field energies will vary somewhat from compound to compound, we cannot be certain of the temperature interval for which the Curie–Weiss expression is a meaningful form with which to fit the data. On the other hand, if the temperature interval is too short, the data will be fit about equally well over some range of T_c and X_0 values, making a determination of these values with any confidence problematic. We fit the data over the intervals 80 to 300, 100 to 300, and 120 to 300 K. The best fits varied somewhat, depending upon the interval used, from $C = 6.53 \times 10^{-3}$ emu K/g, $T_c = 32$ K, and $X_0 = 2.48 \times 10^{-6}$ emu/g over the interval 80 to 300 K to $C = 7.24 \times 10^{-3}$ emu K/g, $T_c = 44$ K, and $X_0 = 1.02 \times 10^{-6}$ emu/g over 120 to 300 K. We note that the T_c values do not reflect exchange interactions only, but also reflect the leading corrections to the susceptibility due to the crystal field splitting of the Nd levels. While we cannot obtain the values of the constants in the Curie–Weiss expression with a high degree of confidence due to the above fitting difficulties, it is clear that a positive X_0 of 1 to 3×10^{-6} is present. If the data are forced to fit an expression with $X_0 = 0.0$ or a $T_c = 0.0$, the goodness of fit to the Curie–Weiss expression over the above temperature intervals is a factor of 4 to 5 poorer (standard deviations increase from 0.2 to above 1%).

The magnetic moment per Nd obtained from the above fits to the Curie–Weiss law vary from 3.61 μ_B (80 to 300 K fit) to 3.80 μ_B (120 to 300 K fit). These values compare favorably with the theoretical moment expected for a free Nd^{3+} ion of 3.62 μ_B. If the

material contained magnetic Ni^{3+} ions, they would contribute to the measured Curie constant as well. If we approximated that nickel moment as a $g = 2$ and $S = 1/2$ moment, then the *minimum* value of C we could obtain would be 8.04×10^{-3} emu K/g, well above the range determined from the fit.

Discussion

Since the structure and nickel valence are the same as those of $LaNiO_3$, and since the unit cell volume is a little smaller in $NdNiO_3$ than that of $LaNiO_3$ (the rhombohedral unit cell volumes are 112.6 and 112.9 $Å^3$, respectively), a metallic band at the Fermi level is expected for $NdNiO_3$. This band should be of Ni e_g parentage (*13*). The bandwidth is primarily determined by the strong O–e_g–O overlap of the oxygen orbitals and the d-orbitals of the Ni^{3+} ion in the slightly distorted octahedral field.

Between 300 and 130 K the resistance decreases with decreasing temperature as expected for a metal. However, the room-temperature resistivity of 1.5×10^{-2} ohm cm is high for a metallic material. A similarly prepared sample of $LaNiO_3$ had a room-temperature resistivity of 4×10^{-3} ohm cm. The lowest reported literature value for the resistivity of $LaNiO_3$ samples sintered at high temperatures is about 1×10^{-3} ohm cm. The minimum metallic conductivity (*13, 14*) expected for the Nd compound, assuming one conduction electron per Ni, would be on the order of 10^{-3} ohm cm, as it is for $LaNiO_3$. It might be that the high value of the resistivity is due to the polycrystalline nature of the sample and the low sintering temperatures. Indeed, combined with the positive value of X_0 and the fact that the value of C is less than expected if Ni^{3+} also had a magnetic moment, it would appear that this compound is indeed a metal, but close to the metal–insulator boundary.

Below 130 K the resistivity increases with decreasing temperature. Figure 4 shows a plot of ln R vs $1/T$. Between 130

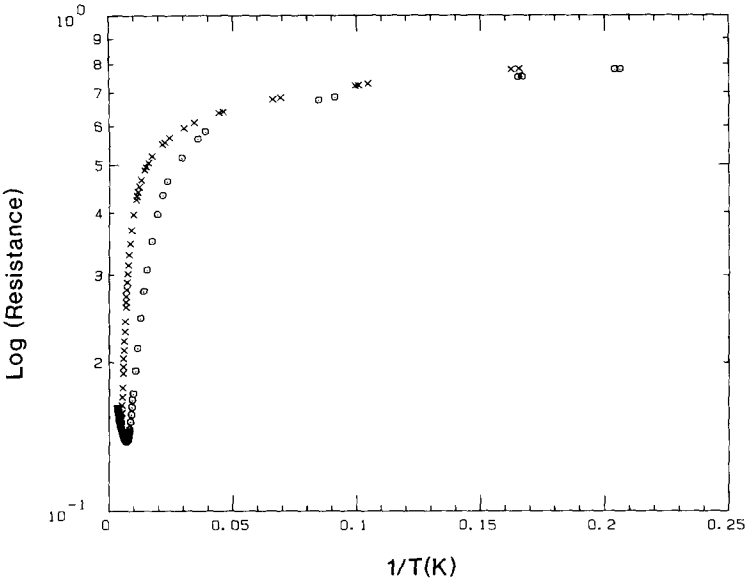

FIG. 4. The logarithm of the resistance versus inverse temperature is used to extract activation energies.

and 50 K the conductivity is thermally activated with an activation energy of 80 K. This behavior is typical of a semiconductor, indicating that $NdNiO_3$ undergoes a metal–semiconductor transition at about 130 K. Below 10 K the data is fit by a much lower activation energy, 5 K. This lower activation energy might be expected for a semiconductor as it changes from intrinsic to extrinsic behavior as the temperature is lowered. It is likely that this "transition" near 130 K is structural in nature, since an obvious hysteresis is seen in the resistivity. Essentially no anomaly is seen in the susceptibility, although the large contribution of the local moment paramagnetism may mask small temperature dependent changes in X_0 that should result from a metal–insulator transition. It is perhaps coincidental that the deviation of the inverse susceptibility from straight line behavior in Fig. 3 also occurs near 130 K, although in a very gradual manner. This possible temperature dependence in X_0 would also cause difficulty in trying to fit the data to the Curie–Weiss susceptibility, although at 130 K X_0 is perhaps only 2 to 5% of the total susceptibility.

A variety of interpretations can be given to the above data. These would include a Mott transition at 130 K or small polaron formation at that same temperature. It is even possible that a transition is driven by the small interaction of the conduction electrons in an almost localized band with the Nd magnetic moments.

A model consistent with the resistivity measurements is based on a Mott–Hubbard metal–insulator transition. The narrow *d*-band of $NdNiO_3$ is half-filled, and at room temperature the conductivity is metallic. We can assume that at 130 K $NdNiO_3$ undergoes an antiferromagnetic transition as in the case of $LaTiO_3$ (*15*). The half-filled band is split into an upper empty band and a lower completely filled band. The energy gap developing from the splitting of the Hubbard bands is responsible for the semiconducting character of the resistivity. However, the changes in the susceptibility due to the antiferromagnetic ordering is masked by the strong paramagnetic signal due to the *f*-electrons of the Nd^{3+} ions.

Another mechanism able to explain the semiconducting behavior below 130 K is polaron formation (*13*). At room temperature, the conductivity of $NdNiO_3$ is above the value of the minimum metallic conductivity (*14*) of 10^{+3} (ohm cm)$^{-1}$. In this limit, the mean free path of the electrons is of the order of the interatomic distance. The electrons move in a diffusive way in the narrow *d*-bands whose width is determined by the uncertainty principle, $W = h/t_s$, where W is the width of the band and t_s is the relaxation time. In the metallic regime between 300 and 130 K the conductivity of $NdNiO_3$ is diffusive. Below 130 K, small polaron formation localizes the electrons and the conductivity behavior is semiconducting. In this temperature domain the relaxation time, t_s, is determined by the phonon-assisted hopping time of the electrons from site to site. The localization of the 3*d*-electrons may be accompanied by a Jahn–Teller distortion, as in the case of $LaMnO_3$ (*16*). A large thermal hysteresis of this lattice distortion could be responsible for the large resistivity hysteresis observed.

With the present polycrystalline samples the resistivity data are not sufficiently convincing to allow detailed comparisons with any particular theory or to discriminate between them.

Summary

$NdNiO_3$ has been prepared in the same structure type as $LaNiO_3$ by a low-temperature synthetic method, without the use of high oxygen pressures as previously used. The magnetic properties show qualitatively the expected behavior of Nd^{3+} in a crystal field. The electrical resistivity is metallic-like at room temperature, but it is about an

order of magnitude higher than the expected minimum metallic conductivity. This may be due to the polycrystalline nature of the material. There is a "transition" to semiconductor-like behavior at about 130 K. Since this transition shows considerable thermal hysteresis, it appears to be a thermodynamically first-order structural transition.

Since the lattice parameters of $NdNiO_3$ are slightly smaller than those of $LaNiO_3$, the bandwidths are expected to be similar. Consequently, $NdNiO_3$ might be expected to be a "normal" metal like $LaNiO_3$. Further studies of $NdNiO_3$, especially if single crystals can be prepared under pressure, are clearly needed to understand the puzzling behavior reported in this work.

References

1. G. Demazeau, A. Marbeuf, M. Pouchard, and P. Hagenmuller, *J. Solid State Chem.* **3,** 582–589 (1971).
2. A. Wold, B. Post, and E. Banks, *J. Amer. Chem. Soc.* **79,** 4911 (1957).
3. A. Wold, R. J. Arnott, and J. B. Goodenough, *J. Appl. Phys.* **29,** 387 (1958).
4. B. Willer and M. Daire, *C.R. Acad. Sci.* **267,** 1483 (1968).
5. M. Pechini, U.S.P. 3, 231 328/1966; M. Vallet-Regi, E. Garcia, and J. M. Gonzales-Calbert, *J. Chem. Soc. Dalton Trans.*, 775 (1988); H. Wang *et al., Inorg. Chem.* **26,** 1476–1481 (1987); S. Davison, K. Smith, R. Kershaw, K. Dwight, and A. Wold, *Mater. Res. Bull.* **22,** 1659–1664 (1987).
6. F. Bertaut and F. Forrat, *J. Phys. Radium* **17,** 129 (1956); MeGaw and Darlington, *Acta Crystallogr. Sect. A* **31,** 161 (1975).
7. V. M. Goldschmidt, "Geochemische Verteilungsgesetze der Elemente," VII, VIII (1927/1928).
8. J. B. Goodenough, J. A. Kafalas, and J. M. Longo, *in* "Preparation Methods in Solid State Chemistry" (P. Hagenmuller, Ed.), Academic Press, New York (1972).
9. Hidehito Obayashi and Tetsuichi Kudo, *Japan. J. Appl. Phys.* **14,** (1975).
10. (*a*) J. C. G. Bunzli, *Inorg. Chem. Acta* **36,** L413 (1979); and references therein; (*b*) R. C. Weast (Ed.), "Handbook of Chemistry & Physics," CRC Press, Boca Raton (1982); (*c*) "Landolt-Bornstein Series," Vol. 2, Sect. 9, "Magnetic Properties I," Springer-Verlag, New York/Berlin (1962).
11. P. W. Selwood, "Magnetochemistry," 2nd ed., p. 186, Interscience, New York (1956).
12. H. Hacker, M. S. Lin, and E. F. Westrum, *in* "Proceedings, IV Conference on Rare Earth Research" (L. Eyring, Ed.), Gordon & Breach, New York (1965).
13. J. B. Goodenough, *Prog. Solid State Chem.* **5,** 145 (1971).
14. N. F. Mott, "Metal–Insulator Transitions," p. 28, Taylor & Francis, London (1974).
15. D. A. Maclean and J. E. Greedan, *Inorg. Chem.* **20,** 1025–1029 (1981).
16. J. B. Goodenough, *Mater. Res. Bull.* **6,** 967 (1971).